Direct Photocatalytic Conversion of Aldehydes to Esters Using Supported Gold Nanoparticles Under Visible Light Irradiation at Room Temperature

ARTICLE *in* THE JOURNAL OF PHYSICAL CHEMISTRY C · JULY 2014

8 AUTHORS, INCLUDING:

Qi Xiao
Queensland University of Technology
14 PUBLICATIONS   146 CITATIONS

SEE PROFILE

Steven E. Bottle
Queensland University of Technology
144 PUBLICATIONS   1,949 CITATIONS

SEE PROFILE

Sarina Sarina
Queensland University of Technology
21 PUBLICATIONS   543 CITATIONS

SEE PROFILE

H. Y. Zhu
Queensland University of Technology
189 PUBLICATIONS   7,399 CITATIONS

SEE PROFILE

Direct Photocatalytic Conversion of Aldehydes to Esters Using Supported Gold Nanoparticles under Visible Light Irradiation at Room Temperature

Yulin Zhang,[†] Qi Xiao,[‡] Yongsheng Bao,[†] Yajing Zhang,[†] Steven Bottle,[‡] Sarina Sarina,[‡] Bao Zhaorigetu,*,[†] and Huaiyong Zhu*,[‡]

[†]College of Chemistry and Environmental Science, Inner Mongolia Key Laboratory of Green Catalysis, Inner Mongolia Normal University, Hohhot, Inner Mongolia 010022, China

[‡]School of Chemistry, Physics, and Mechanical Engineering, Queensland University of Technology, Brisbane, QLD 4001, Australia

Ⓢ *Supporting Information*

ABSTRACT: Visible light can drive esterification from aldehydes and alcohols using supported gold nanoparticles (Au/Al$_2$O$_3$) as photocatalysts at ambient temperatures. The gold nanoparticles (AuNPs) absorb visible light due to the localized surface plasmon resonance (LSPR) effect, and the conduction electrons of the AuNPs gain the energy of the incident light. The energetic electrons, which concentrate at the NP surface, facilitate the activation of a range of aldehyde and alcohol substrates. The photocatalytic efficiencies strongly depend on the Au loading, particle sizes of the AuNPs, irradiance, and wavelength of the light irradiation. Finally, a plausible reaction mechanism was proposed, and the Au/Al$_2$O$_3$ catalysts can be reused several times without significantly losing activity. The knowledge acquired in this study may inspire further studies in new efficient recyclable photocatalysts and a wide range of organic synthesis driven by sunlight.
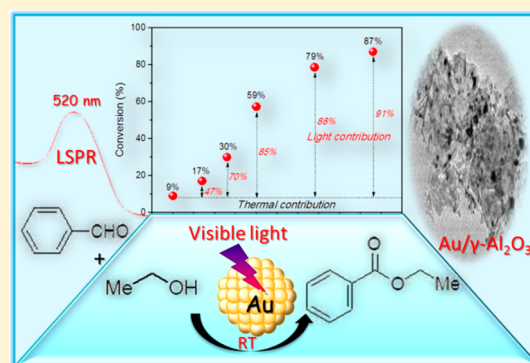
INTRODUCTION

The development of new methodologies for the synthesis of esters has attracted broad interest of chemists due to the fundamental significance and widespread use of these compounds. Traditionally, the most common strategy for the preparation of carboxylic acid ester derivatives under mild conditions usually involves the stoichiometric activation of the parent acid as an acyl halide, anhydride, or activated ester amenable to subsequent nucleophilic substitution.[1] An interesting and potentially valuable alternative transformation in the synthesis of ester derivatives is the oxidative esterification of aldehydes under mild conditions.[2−4] However, these one-pot conventional methods reported require the use of stoichiometric heavy-metal oxidants such as KMnO$_4$,[5] CrO$_3$,[6] and highly reactive hydrogen peroxide,[7] oxone,[8] *N*-iodosuccinimide,[9] or other transition-metal catalysts.[10−15] Esterification of benzaldehyde and alcohols with a wide variety of metal catalysts such as Ru, Cu, Pd, and Au have also been explored; however, these approaches commonly require the use of base and harsh conditions (elevated temperature and O$_2$) to achieve high yields.[16−18] Nonetheless, from a "Green Chemistry" point of view, the use of heterogeneous metal catalysts to achieve oxidation and esterification remains attractive as a cost-effective and efficient means to generate esters from aldehydes and alcohols with minimal hazardous waste production.

Photocatalysis is of particular interest in green chemical science because it combines the efficiency of catalysis with the potential use of sunlight.[19] Photocatalysis driven by sunlight is an ideal process, as a result of the abundance of sunlight, low environmental impact, and sustainability. Recently, visible light driven photocatalysis has shown great potential in organic synthesis.[20−25] It is well-known that AuNPs can strongly absorb visible light due to localized surface plasmon resonance (LSPR) effect.[26,27] The LSPR effect is the collective oscillation of conduction electrons in the NPs, which resonate with the electromagnetic field of the incident light when the conduction electrons gain the energy of the incident photons. AuNPs also absorb UV light, which induces interband electron excitation as these higher energy photons excite individual conduction electrons of AuNPs to high energy levels.[28,29] The resultant excited electrons arising from the LSPR effect and interband transitions can induce chemical reactions of molecules bound to the surface of AuNPs.[27−29] In this context, AuNPs are very attractive if they can generate esters from aldehydes and alcohols under visible light irradiation. Such a photocatalytic process controlled at ambient conditions has the potential to

deliver an efficient synthesis of esters via a controlled, simplified, and greener process.

In the present study, we prepared a series of supported AuNP photocatalysts, in which AuNPs were loaded on several support materials or the size of the supported AuNPs were controlled to be different. These photocatalysts were found to be efficient for catalyzing esterifications from many aldehydes and alcohols under visible light irradiation. The photocatalytic reactions were conducted under moderate conditions: air atmosphere, ambient temperatures, and base free. Au/Al_2O_3 catalyst with an AuNP mean diameter of 4.1 nm exhibited the best performance. Moreover, the catalysts maintained a high activity after several reuse—recover cycles. The intensity and wavelength of the irradiation have important influence on the catalytic reaction. The reaction conversion increased with the increasing light intensity. Evidently, the visible light drove the reaction, and we found that the light with wavelengths in the range between 400 and 650 nm make the main contribution to the conversion. A tentative mechanism was proposed based on the experimental analysis and relevant literatures.

■ EXPERIMENTAL SECTION

Catalyst Preparation. The AuNPs on γ-Al_2O_3 and other supports were prepared by an impregnation-reduction method.[27] For example, 3 wt % Au/Al_2O_3 catalyst was prepared by the following procedure: 1.0 g of γ-Al_2O_3 powder was dispersed into 100 mL of deionized water, followed by adding 16.8 mL of 0.01 M $HAuCl_4$ aqueous solution while magnetically stirring. One milliliter of 0.03 M L-lysine was added with vigorous stirring. Then 0.1 M NaOH aqueous solution was added into the mixture to adjust the pH to 7. To this suspension, 4 mL of 0.35 M $NaBH_4$ solution was added dropwise in 10 min. The mixture was aged for 24 h, and then the solid was separated, washed with water (4 times) and ethanol (once), and dried at 80 °C. The dried solid was used directly as the catalyst. Catalysts with other supports were prepared in a similar method. For the preparation of Au/Al_2O_3 catalysts with different particle sizes, the methods were also similar but with different amounts of L-lysine solution. Au/Al_2O_3_5.7 catalyst, 4 mL of 0.53 M L-lysine was added, and after adding $NaBH_4$ solution, the pH value was adjusted to 9 by adding 4 mL of 0.3 M HCl solution; Au/Al_2O_3_6.2 catalyst, no L-lysine solution was added. The other reaction conditions were kept identical.

Activity Test. The reaction was conducted in a quartz tube with a magnetic stirrer and illuminated with a halogen tungsten lamp. The reaction temperature was controlled by an air-conditioner in a closed box. The light intensity in the reaction position was set at 0.34 W·cm^{-2} and could be adjusted by changing the distance between the reactor and the light source. In the reactions to determine the light—intensity dependence, a photometer was used to measure the light intensity. The wavelength range of the light irradiation was tuned by using various optical low pass glass filters to block light below specific cutoff wavelengths. For example, without any filters, light with wavelengths between 400—800 nm illuminated the system; a filter could be applied to block the wavelengths shorter than 490 nm, and then the wavelengths between 490—800 nm illuminated the system.

Catalytic esterification of benzaldehyde with alcohol to ethyl benzoate was used as the model reaction. Typically, benzaldehyde (0.5 mmol) and photocatalyst (30 mg) were added into 5 mL ethanol. The reaction flask was irradiated with

magnetic stirring using the halogen tungsten lamp (wavelength in the range of 400—750 nm) as the visible light source under air atmosphere.

The products were analyzed by GC (Shimadzu GC-2014) with a HP-5 capillary column (50 m length, 0.25 mm internal diameter, and 0.25 μm film thickness). Column temperature ranged from 170 to 210 °C (10 °C/min), the injector and flame ionization detector temperatures were kept at 300 °C for product analysis. The products were identified by comparison with known standard samples and GC—MS analysis (Thermo DSQ with a DB-5 column).

Catalysts recycle experiment: after each reaction cycle, the solvent, substrate, and products were removed by centrifugation; the separated catalyst was washed thoroughly twice with water and then washed twice with ethanol followed by centrifugal separation and drying at 80 °C for 10 h. The resultant sample was used for recycle.

■ RESULTS AND DISCUSSION

In this study, to explore the possibility of driving the esterification with visible light, we prepared a series of AuNPs with different supports. The AuNPs on γ-Al_2O_3 (Au/Al_2O_3) and other supports (Au/CeO_2 and Au/TiO_2) were prepared by the impregnation—reduction method.[16] The detailed methodology is described in the experimental section. Figure 1a shows
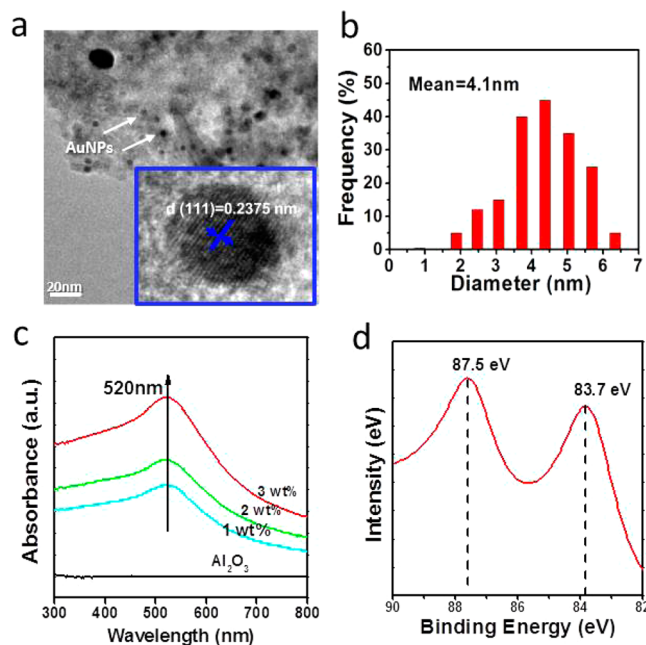

Figure 1. (a) TEM images of the Au/Al_2O_3 supported nanoparticles, the length of the scale bars in the images is 20 nm. The insert in panel a is a high-resolution TEM image; (b) Au particle size distribution of Au/Al_2O_3 based on the statistical analysis from TEM images (by measuring >200 isolate particles in the images of the sample); (c) UV—vis diffuse reflectance spectra of Au/Al_2O_3 with various amounts of gold loads (1, 2, and 3 wt %); (d) XPS spectra of Au/Al_2O_3.

the transmission electron microscopy (TEM) images of Au/Al_2O_3 supported nanoparticles. The TEM images of Au/CeO_2 and Au/TiO_2 analogues are given in Figure S1 (Supporting Information). The AuNPs are well dispersed and have narrow size distributions (Figure 1b). The average of mean diameters of the AuNPs supported on Al_2O_3 is 4.1 nm. The morphology and structure of the AuNPs was determined from high-

resolution TEM (insert in Figure 1a). The AuNPs are spherical and the Au (111) plane can be clearly observed in the HRTEM image.

The UV−visible spectra of Au/Al$_2$O$_3$ catalysts are shown in Figure 1c. An absorption band at about 520 nm is observed in the UV/vis spectra of the photocatalysts, which is the characteristic LSPR absorption by AuNPs. Increasing the Au loading can increase the absorption intensity. The Au/Al$_2$O$_3$ combination gives a stronger intensity compared to AuNPs on other supports (Figure S2, Supporting Information), indicating a stronger LSPR effect for Au/Al$_2$O$_3$. The spectra of Au/Al$_2$O$_3$ with various amounts of gold loadings demonstrate that the amount of light absorption increases with the increasing levels of the AuNPs present on the support. The XPS (X-ray photoelectron spectroscopy) spectrum of Au/Al$_2$O$_3$ shows the Au 4f$_{7/2}$ core level at a binding energy of 83.7 eV (Figure 1d), which indicates that AuNPs on the supports exist in the metallic state.

As the light absorption property and the catalytic activity of AuNPs strongly depend on the sizes of AuNPs, we also prepared Au/Al$_2$O$_3$ samples with different AuNP mean diameters by tuning the concentration of lysine solution during the reduction procedure; the detailed method is provided in the experimental section. The TEM images of the samples with mean AuNP diameters of 6.2 and 5.7 nm, are shown in Figure 2c,d, respectively. We denoted these two Au/Al$_2$O$_3$ catalysts
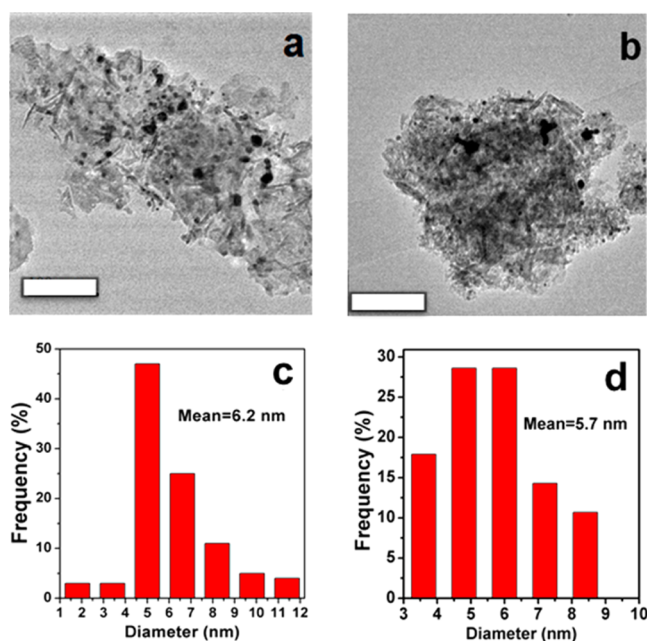

Figure 2. (a,b) TEM images of the larger Au/Al$_2$O$_3$ nanoparticles, the length of the scale bar in the images is 100 nm; (c,d) Au particle size distribution for Au/Al$_2$O$_3$ shown in panels a and b, respectively; he size distributions were obtained from TEM images by counting >200 isolate gold particles in the images of a sample.

Au/Al$_2$O$_3$_5.7 and Au/Al$_2$O$_3$_6.2, respectively. As shown in Figure 3a, the LSPR absorption peaks of the two samples with large mean AuNP diameters red-shift to 530 and 539 nm, respectively. It has been known that the increase in particle sizes of AuNPs in the samples results in a red-shift of the LSPR absorption peak.[30]

X-ray diffraction (XRD) patterns of Au/Al$_2$O$_3$ catalysts with various particle sizes are shown in Figure 3b, the peaks around

2θ = 38.2, 44.5, and 64.6 are observed and assigned to the characteristic diffraction peaks of the (111), (200), and (220) planes of the AuNPs in the samples, respectively.[31] The reflection peaks weaken as the sizes of the AuNPs decrease, no evident peaks from gold crystals were observed in the samples with mean AuNP diameters of 4.1 and 5.7 nm.

The Brauner−Emmet−Teller (BET) specific surface areas of the samples were derived from N$_2$ physical sorption data of the samples using the BET method, which are similar to that of the Al$_2$O$_3$ support (Table 1). The γ-Al$_2$O$_3$ support has a large specific surface area, and loading a small amount of the AuNPs, ∼ 3 wt % as shown below, does not cause significant change in the specific surface area of samples. The amount of surface acidity of the samples was measured by NH$_3$ temperature-programmed desorption (NH$_3$-TPD), and it was found that the loading of AuNPs slightly reduced the surface acidity. Nonetheless, there is no substantial difference in the surface acidity between the Au/Al$_2$O$_3$ catalysts. The amounts of Au loading in the samples were determined by atomic absorption spectrophotometer (AAS), and the three samples have nearly the same Au loading (3 wt %).

A series of samples of AuNPs supported on TiO$_2$, CeO$_2$, and Al$_2$O$_3$ were also prepared and investigated to see the influence of the support materials on the performance of the photo-catalysts (Table 2). After 12 h of visible light irradiation, the AuNPs on TiO$_2$, CeO$_2$, and Al$_2$O$_3$ converted 27.1%, 39.9%, and 78.3% of benzaldehyde, respectively. Moreover, Au/Al$_2$O$_3$ catalysts with larger particle size (Au/Al$_2$O$_3$_5.7 and Au/Al$_2$O$_3$_6.2) exhibited much lower activity and selectivity. In the dark, no conversion above 5% was observed with any of these catalysts. Blank experiments under otherwise identical conditions but without AuNPs (reaction mixture with the oxide supports TiO$_2$, CeO$_2$, and Al$_2$O$_3$ only) were conducted. No conversion above 3% was observed. We also found that the photocatalytic efficiency was significantly influenced by gold loading and that the catalyst with 3 wt % Au exhibited the best performance (Table S1, Supporting Information).

Light intensity and wavelength are important irradiation energy parameters, and hence, they are the critical factors influencing the performance of photocatalyst in reactions.[23−25] For example, the TOF of Au/Al$_2$O$_3$ catalyst for the esterification under light irradiation is 7.2 h^{-1}, which is nearly 18-fold of that in the dark reaction (0.4 h^{-1}). Notably, among the AuNPs supported on various supports tested, the Au/Al$_2$O$_3$ catalyst, which has a stronger absorbance (compared with Au/TiO$_2$ and Au/CeO$_2$ as shown in Figure S2, Supporting Information), showed the highest catalytic performance for the esterification of benzaldehyde with ethanol. To further clarify the influence of light intensity, we reduced the irradiation intensity from 0.48 to 0.34, 0.20, 0.13, and finally 0.07 W·cm^{-2}, while other experimental conditions were kept unchanged. As expected the conversion rates decreased correspondingly (Figure 4). The light induced enhancement of the catalytic conversion was calculated by subtracting the observed conversion of a reaction performed in the dark from the conversion observed under light irradiation performed at the same temperature (red percentage numbers in Figure 4). These results clearly show that higher light intensities give rise to a greater light enhanced contribution to the total conversion rate. Such an effect reveals that the light intensity plays an important role in the photocatalytic esterification. Under visible light irradiation, higher intensities excite more energetic electrons of the AuNPs and enhance the interaction with reactants absorbed
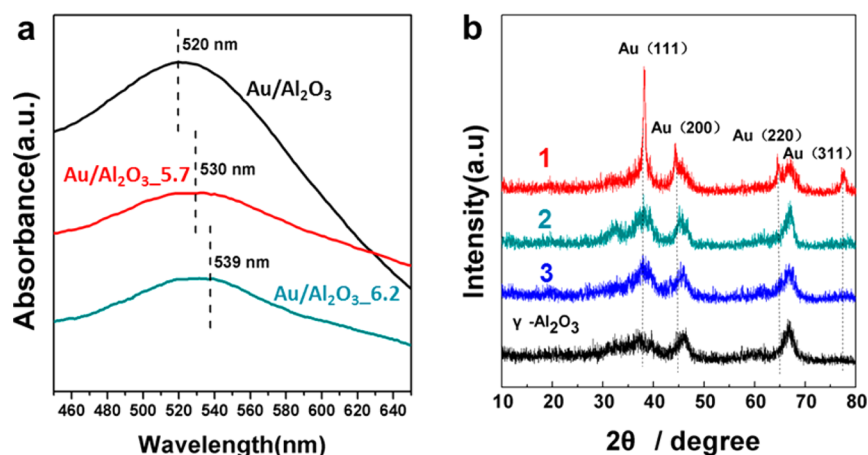
Figure 3. (a) UV−vis diffuse reflectance spectra of Au/Al$_2$O$_3$ catalysts with various particle sizes; (b) X-ray diffraction (XRD) patterns of Au/Al$_2$O$_3$ catalysts with various particle sizes (1, Au/Al$_2$O$_3$_6.2; 2, Au/Al$_2$O$_3$_5.7; 3, Au/Al$_2$O$_3$).

Table 1. Characterization Results of BET, NH$_3$-TPD and AAS of the Au/Al$_2$O$_3$ Catalysts with Different Particle Sizes

catalysts	S_{BET} (m^2/g)	NH$_3$ desorbed (mmol/g$_{cat}$)	Au loading[a] (wt %)
Au/Al$_2$O$_3$_6.2	204.8	0.38	3.3
Au/Al$_2$O$_3$_5.7	196.0	0.39	3.1
Au/Al$_2$O$_3$	201.3	0.39	2.9
γ-Al$_2$O$_3$	204.1	0.41	

[a]The Au loading was determined by an atomic absorption spectrophotometer (AAS).

Table 2. Photocatalytic Esterification of Benzaldehyde with Ethanol Using Supported Au-NPs[a]

catalysts	visible light			dark		
	conv (%)	sel (%)	TOF (h^{-1})	conv (%)	sel (%)	TOF (h^{-1})
Au/Al$_2$O$_3$	**78.3**	**99.4**	**7.2**	**4.4**	**99.7**	**0.4**
Au/Al$_2$O$_3$_6.2	43.1	20.7	0.8	3.5	24.3	0.1
Au/Al$_2$O$_3$_5.7	44.3	81.0	3.3	4.6	73.6	0.3
Au/CeO$_2$	39.9	94.3	3.5	4.5	99.1	0.4
Au/TiO$_2$	27.1	87.2	2.2	4.6	89.1	0.3

[a]Reaction conditions: benzaldehyde (0.5 mmol) and Au catalyst (30 mg) were added into ethanol (5 mL); the reaction flask stirred magnetically was irradiated with the halogen tungsten lamp (wavelength in the range of 400−750 nm, light intensity 0.34 W·cm^{-2}) as the visible light source under air atmosphere at room temperature. The reaction was conducted for 12 h. The reaction conversion and selectivity were determined by GC. The TOF (turnover frequency) values were calculated on the basis of the amount of Au metal.

on the AuNPs. These results demonstrate clearly that the esterification reaction was driven by visible light.

To determine the effect of wavelength, we applied various optical low pass filters to block light below specific cutoff wavelengths. The dependence of the catalytic performance on wavelength range for the esterification reaction is illustrated in Figure 5. When wavelengths between 400−800 nm were used to illuminate the system, a conversion efficiency of 79% for the reaction of benzaldehyde was observed. Applying a filter that limited the transmitted wavelengths to 510−800 nm (while the irradiation intensity on the reactor was kept unchanged) decreased the conversion efficiency to 69%. When the
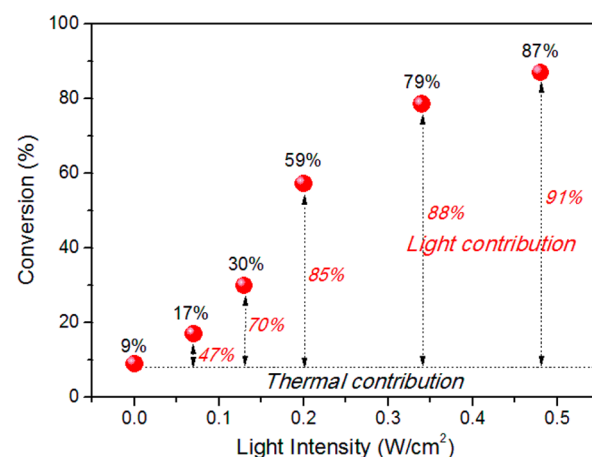

Figure 4. Effect of light intensity on esterification of benzaldehyde with Au/Al$_2$O$_3$.
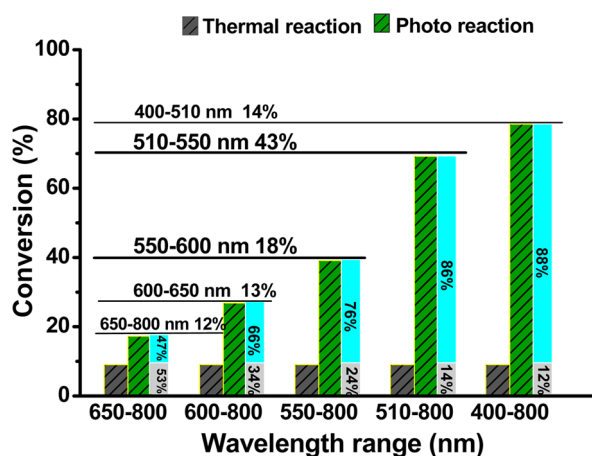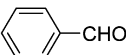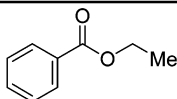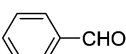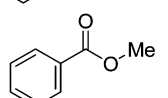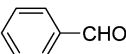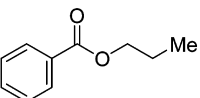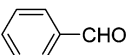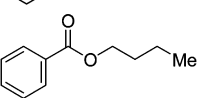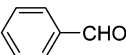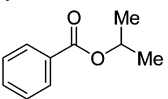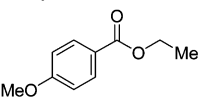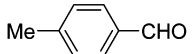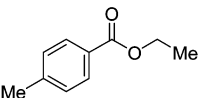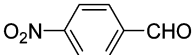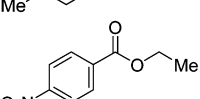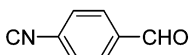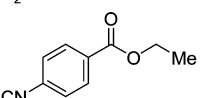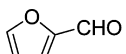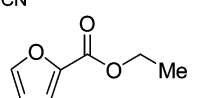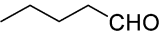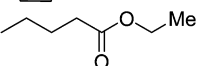

Figure 5. Effect of light wavelength on esterification of benzaldehyde with Au/Al$_2$O$_3$.

wavelength of the irradiation was further restricted (to 550−800 nm), the conversion decreased to only 39%. Filtering the incident light to limit the irradiation wavelength to 600−800 nm further decreased the conversion to 27%. In the dark, the reaction conversion at this temperature was only 9%. Irradiating the system with light of wavelength longer than 650 nm or

Table 3. One-Pot Esterification of Various Aldehydes and Alcohols over Au/Al$_2$O$_3$ by Visible Light Irradiation[a]

Entry	Aldehyde	Alcohol	Product	Yield (%)	TOF (h^{-1})
1	⬡–CHO	ethanol	(ethyl benzoate)	78.3	7.2
2	⬡–CHO	methanol	(methyl benzoate)	79.4	7.3
3	⬡–CHO	propyl alcohol	(propyl benzoate)	78.0	7.2
4	⬡–CHO	butyl alcohol	(butyl benzoate)	78.9	7.3
5	⬡–CHO	isopropyl alcohol	(isopropyl benzoate)	61.7	5.7
6	MeO–⬡–CHO	ethanol	(ethyl 4-methoxybenzoate)	85.5	7.9
7	Me–⬡–CHO	ethanol	(ethyl 4-methylbenzoate)	80.8	7.5
8	O$_2$N–⬡–CHO	ethanol	(ethyl 4-nitrobenzoate)	63.7	5.9
9	CN–⬡–CHO	ethanol	(ethyl 4-cyanobenzoate)	59.3	5.5
10	(furyl)–CHO	ethanol	(ethyl furan-2-carboxylate)	47.1	4.4
11	(pentyl)–CHO	ethanol	(ethyl pentanoate)	59.9	5.5

[a]Reaction conditions: aldehyde (0.5 mmol) and Au catalyst (30 mg) were added into alcohol (5 mL); the reaction flask stirred magnetically was irradiated with the halogen tungsten lamp (wavelength in the range of 400−750 nm, light intensity 0.34 W·cm^{-2}) as the visible light source under air atmosphere at room temperature. The reaction was conducted for 12 h. The reaction conversion and selectivity were determined by GC. The TOF values were calculated on the basis of the amount of Au metal.

shorter than 510 nm produces little change to the reaction. The contribution to the conversion of the benzaldehyde using the light of wavelength 400−650 nm was 88% of the total conversion. Similarly, we can calculate the contribution to the conversion efficiency for any of the specific wavelength ranges used. As illustrated in Figure 5, light in the wavelength ranges 510−550 and 550−600 nm account for 43% and 18%, respectively, of the light induced conversion (conversion difference of visible-light enhanced reaction and the reaction in the dark), while light in the wavelength ranges of 650−800 nm contribute the remaining 12%. Given that the LSPR peak of AuNPs is in the wavelength range between 500 and 600 nm, these results suggest that for the Au/Al$_2$O$_3$ photocatalysts it is the gold that harvests visible light and that the LSPR effect plays a critical role in enhancing the reaction activity in the catalyzed reactions.

The scope of the method to generate a broad range of esters was investigated with a variety of aldehydes and alcohols using Au/Al$_2$O$_3$ as the photocatalyst. First, we used benzaldehyde to react with different alcohols, as shown in Table 3 (entries 1−5). Not only ethanol provided the desired products in high yield but also methanol, n-propyl alcohol, 1-butanol, and isopropyl alcohol gave the corresponding benzoate esters under visible light irradiation. When the reactions were conducted in the dark with all other experimental conditions remaining identical, the yields of the esters were less than 10% in all cases.

Various substituted benzaldehydes were successfully converted to the corresponding esters in good to moderate yields. The targeted ester was isolated in 86% yield when p-methoxybenzaldehyde (which possesses a strongly electron-donating group) was used as the substrate. When a methyl group was present, substitution in the para position led to good results. Strongly electron-withdrawing groups such as −NO$_2$ and −CN could also be tolerated under the standard conditions (Table 3, entries 8 and 9) but gave reduced yields (64% and 59%) of the desired ester. Even reactive heterocycles such as

Scheme 1. Proposed Mechanism for the Esterification of Benzaldehyde with Alcohol Using AuNPs under Light Irradiation
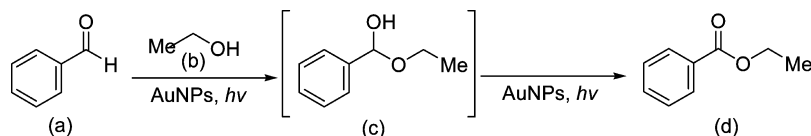
furfural aldehyde could be successfully converted to the corresponding esters in modest yield (47%, Table 3, entry 10). Apart from furfural, the methodology was also successful in converting other nonaromatic aldehydes to the corresponding esters: a long-chain aliphatic aldehyde, valeraldehyde, was used in the reaction, and the desired product was obtained in moderate yield (60%, Table 3, entry 11). These results demonstrate that under visible light irradiation, Au/Al_2O_3 can be applied to both benzylic aldehydes and aliphatic aldehydes to efficiently convert them to the ester derivaives. Notably, both electron-rich and electron-poor benzylic aldehydes were suitable for this transformation using light-induced AuNP catalysis.

The contribution of visible light irradiation to reducing the apparent activation energies of the reactions was also investigated. The difference between the apparent activation energies of the two processes demonstrates the contribution of light irradiation to reducing the apparent activation energy. The results in Figure S3, Supporting Information, show that the activation energy is 30.4 $kJ·mol^{-1}$ for the photocatalytic reduction and 63.1 $kJ·mol^{-1}$ for the thermal reduction. The substantial difference between the two activation energies (32.7 $kJ·mol^{-1}$) reveals the significant contribution light irradiation plays in activating the reaction.

To gain some insight into the mechanism of the reaction process, we investigated if molecular oxygen plays a role in the reaction progress. When an argon atmosphere is used to limit oxygen availability (with all other reaction conditions kept identical), no ester products were detected. This demonstrates the essential role of oxygen in the reaction. Mechanistically it is possible that the aldehydes are oxidized with O_2 to give the corresponding acid, which then reacts with alcohol to give the ester. However, no carboxylic acids could be detected by GC in the present study. Furthermore, when benzoic acid is used as the reaction substrate instead of benzaldehyde under identical conditions, no ethyl benzoate was formed. These results suggest that the aldehydes are not converted to the corresponding acids and that another mechanism is involved.

The mechanism proposed in Scheme 1 is consistent with recent relevant literature where an oxidant converts a hemiacetal intermediate to the ester.[18,32−34] In this case the benzaldehyde molecule is adsorbed on the AuNP surface because the AuNP surface has a strong binding affinity to the aromatic moiety. The oxidative esterification reaction may then proceed through a condensation reaction between benzaldehyde (a) and alcohol (b), which results in the formation of hemiacetal intermediate (c), followed by oxidative dehydrogenation to give the corresponding ester (d). The light excited high-energy electrons of AuNPs may facilitate the condensation step through electron transfer and recombination. However, the LSPR effect also enhances the local electromagnetic fields near rough surfaces of the AuNPs, and this could enhance the carbonyl dipole to increase the reactivity toward nucleophilic attack by the alcohol to give the hemiacetal. It could also assist the oxidative dehydrogenation when the reactant molecules are adsorbed on the surface of AuNPs. Whatever the mechanism

that is involved with the reaction, the catalytic process of the AuNPs also clearly depends on the energy of the excited electrons in AuNPs under light irradiation, which can be tuned by light intensity and wavelength as discussed previously.

A key attraction to heterogeneous catalysis is the possibility of catalyst recycling. To address this issue, we carried out a series of experiments using esterification of benzaldehyde with alcohol under light irradiation to demonstrate the recyclability of Au/Al_2O_3 catalyst. Briefly, after each reaction cycle, by removal of the solvent, substrate, and products by centrifugation, the separated Au/Al_2O_3 catalyst was washed thoroughly by water and ethanol twice and dried for subsequent reactions. As shown in Figure 6, the catalyst was reused for several cycles,
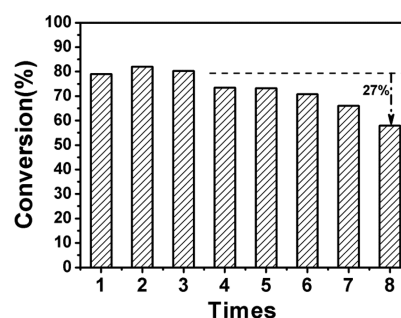

Figure 6. Photocatalytic activity of Au/Al_2O_3 catalyst after being reused 8 times.

with only 27% reduction of activity after 8 runs. From the typical TEM image of the Au/Al_2O_3 catalyst after 8 catalytic cycles (Figure 7), the AuNPs still distribute evenly on the
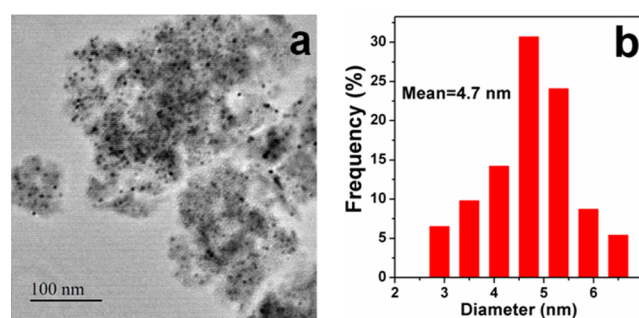

Figure 7. (a) Representative TEM image of Au/Al_2O_3 catalyst after 8 catalytic cycles and (b) Au particle size distribution determined from TEM images by measuring >200 isolate particles from images captured from distinct quadrants of the grid.

Al_2O_3 surface, no apparent agglomeration was observed. We did note a slight increase in the average size of the particles after being cycled 8 times (Figure 7b), and this may result in a concomitant decrease in surface area, which can further decrease the catalytic activity on the basis of available Au on the support surface.[35]

CONCLUSIONS

In conclusion, it was found for the first time that visible light can drive esterification from aldehydes and alcohols using AuNPs at ambient temperatures. The dependence of activity on light intensity and wavelength indicated that light absorption of AuNPs is responsible for the observed photocatalytic activity. Light irradiation can drive various aldehydes (both aromatic aliphatic aldehydes) and alcohols into the corresponding esters in high yields. The knowledge acquired in this study may inspire further studies on new efficient photocatalysts for a wide range of organic syntheses driven by sunlight.

ASSOCIATED CONTENT

Supporting Information

Chemicals, catalyst characterization, Figures S1—S3, Table S1, and GCMS data. This material is available free of charge via the Internet at http://pubs.acs.org.

AUTHOR INFORMATION

Corresponding Authors

*(B.Z.) E-mail: zrgt@imnu.edu.cn.
*(H.Z.) E-mail: hy.zhu@qut.edu.au.

Notes

The authors declare no competing financial interest.

ACKNOWLEDGMENTS

REFERENCES

(1) Larock, R. C. *Comprehensive Organic Transformations: A Guide to Functional Group Preparation*; VCH: New York, 1989; pp 840−841.

(2) De Sarkar, S.; Grimme, S.; Studer, A. NHC Catalyzed Oxidations of Aldehydes to Esters: Chemoselective Acylation of Alcohols in Presence of Amines. *J. Am. Chem. Soc.* **2010**, *132*, 1190−1191.

(3) Tschaen, B. A.; Schmink, J. R.; Molander, G. A. Pd-Catalyzed Aldehyde to Ester Conversion: A Hydrogen Transfer Approach. *Org. Lett.* **2013**, *15*, 500−503.

(4) Reddy, R. S.; Rosa, J. N.; Veiros, L. F.; Caddick, S.; Gois, P. M. P. NHC/Iron Cooperative Catalysis: Aerobic Oxidative Esterification of Aldehydes with Phenols. *Org. Biomol. Chem.* **2011**, *9*, 3126−3129.

(5) Abiko, A.; Roberts, J. C.; Takemasa, T.; Masamune, S. $KMnO_4$ Revisited: Oxidation of Aldehydes to Carboxylic Acids in the tert-Butyl Alcohol−Aqueous NaH_2PO_4 System. *Tetrahedron Lett.* **1986**, *27*, 4537−4540.

(6) Garegg, P. J.; Olsson, L.; Oscarson, S. Synthesis of Methyl (Ethyl 2-O-acyl-3,4-di-O-benzyl-1-thio-β-D-glucopyranosid)uronates and Evaluation of Their Use as Reactive β-Selective Glucuronic Acid Donors. *J. Org. Chem.* **1995**, *60*, 2200−2204.

(7) Qian, G.; Zhao, R.; Ji, D.; Lu, G.; Qi, Y.; Suo, J. Facile Oxidation of Aldehydes to Esters Using S SnO_2/SBA-1-H_2O_2. *Chem. Lett.* **2004**, *33*, 834−835.

(8) Travis, B. R.; Sivakumar, M.; Hollist, G. O.; Borhan, B. Facile Oxidation of Aldehydes to Acids and Esters with Oxone. *Org. Lett.* **2003**, *5*, 1031−1034.

(9) McDonald, C.; Holcomb, H.; Kennedy, K.; Kirkpatrick, E.; Leathers, T.; Vanemon, P. The N-Iodosuccinimide-Mediated Conversion of Aldehydes to Methyl Esters. *J. Org. Chem.* **1989**, *54*, 1213−1215.

(10) Gopinah, R.; Barkakaty, B.; Talukdar, B.; Patel, B. K. Peroxovanadium-Catalyzed Oxidative Esterification of Aldehydes. *J. Org. Chem.* **2003**, *68*, 2944−2947.

(11) Grigg, R.; Mitchell, T. R. B.; Sutthivaiyakit, S. Oxidation of Alcohols by Transition Metal Complexes—iv: The Rhodium Catalyzed Synthesis of Esters from Aldehydes and Alcohols. *Tetrahedron* **1981**, *37*, 4313−4319.

(12) Yoo, W. J.; Li, C. J. Copper-Catalyzed Oxidative Esterification of Alcohols with Aldehydes Activated by Lewis Acids. *Tetrahedron Lett.* **2007**, *48*, 1033−1035.

(13) Kiyooka, S. I.; Wada, Y.; Ueno, M.; Yokoyama, T.; Yokoyama, R. [IrCl(cod)]₂-catalyzed Direct Oxidative Esterification of Aldehydes with Alcohols. *Tetrahedron* **2007**, *63*, 12695−12701.

(14) Bolm, C.; Legros, J.; Le Paih, J.; Zani, L. Iron-Catalyzed Reactions in Organic Synthesis. *Chem. Rev.* **2004**, *104*, 6217−6254.

(15) Enthaler, S.; Junge, K.; Beller, M. Sustainable Metal Catalysis with Iron: From Rust to a Rising Star? *Angew. Chem., Int. Ed.* **2008**, *47*, 3317−3321.

(16) Rout, S. K.; Guin, S.; Ghara, K. K.; Banerjee, A.; Patel, B. K. Copper Catalyzed Oxidative Esterification of Aldehydes with Alkylbenzenes via Cross Dehydrogenative Coupling. *Org. Lett.* **2012**, *14*, 3982−3985.

(17) Liu, C.; Tang, S.; Zheng, L. W.; Liu, D.; Zhang, H.; Lei, A. W. Covalently Bound Benzyl Ligand Promotes Selective Palladium-Catalyzed Oxidative Esterification of Aldehydes with Alcohols. *Angew. Chem., Int. Ed.* **2012**, *51*, 5662−5666.

(18) Liu, P.; Li, C.; Hensen, E. J. M. Efficient Tandem Synthesis of Methyl Esters and Imines by Using Versatile Hydrotalcite-Supported Gold Nanoparticles. *Chem.—Eur. J.* **2012**, *18*, 12122−12129.

(19) Fagnoni, M.; Dondi, D.; Ravelli, D.; Albini, A. Photocatalysis for the Formation of the C−C Bond. *Chem. Rev.* **2007**, *107*, 2725−2756.

(20) Nicewicz, D. A.; MacMillan, D. W. C. Merging Photoredox Catalysis with Organocatalysis: The Direct Asymmetric Alkylation of Aldehydes. *Science* **2008**, *322*, 77−80.

(21) Shih, H. W.; Vander Wal, M. N.; Grange, R. L.; MacMillan, D. W. C. Enantioselective r-Benzylation of Aldehydes via Photoredox Organocatalysis. *J. Am. Chem. Soc.* **2010**, *132*, 13600−13603.

(22) Pham, P. V.; Nagib, D. A.; MacMillan, D. W. C. Photoredox Catalysis: A Mild, Operationally Simple Approach to the Synthesis of α-Trifluoromethyl Carbonyl Compounds. *Angew. Chem., Int. Ed.* **2011**, *50*, 6119−6122.

(23) Sarina, S.; Zhu, H.; Jaatinen, E.; Xiao, Q.; Liu, H.; Jia, J.; Chen, C.; Zhao, J. Enhancing Catalytic Performance of Palladium in Gold and Palladium Alloy Nanoparticles for Organic Synthesis Reactions Through Visible Light Irradiation at Ambient Temperatures. *J. Am. Chem. Soc.* **2013**, *135*, 5793−5801.

(24) Sarina, S.; Zhu, H. Y.; Xiao, Q.; Jaatinen, E.; Jia, J.; Huang, Y.; Zheng, Z.; Wu, H. Viable Photocatalysts Under Solar-Spectrum Irradiation: Nonplasmonic Metal Nanoparticles. *Angew. Chem., Int. Ed.* **2014**, *53*, 2935−2940.

(25) Xiao, Q.; Sarina, S.; Bo, A.; Jia, J.; Liu, H.; Arnold, D. P.; Huang, Y.; Wu, H.; Zhu, H. Visible Light Driven Cross-Coupling Reactions at Lower Temperatures Using a Photocatalyst of Palladium and Gold Alloy Nanoparticles. *ACS Catal.* **2014**, *4*, 1725−1734.

(26) Chen, X.; Zhu, H. Y.; Zhao, J. C.; Zheng, Z. F.; Gao, X. P. Visible-Light-Driven Oxidation of Organic Contaminants in Air with Gold Nanoparticle Catalysts on Oxide Supports. *Angew. Chem., Int. Ed.* **2008**, *47*, 5353−5356.

(27) Zhu, H. Y.; Ke, X. B.; Yang, X. Z.; Sarina, S.; W. Liu, H. Reduction of Nitroaromatic Compounds on Supported Gold Nanoparticles by Visible and Ultraviolet Light. *Angew. Chem., Int. Ed.* **2010**, *49*, 9657−9661.

(28) Sarina, S.; Waclawik, E. R.; Zhu, H. Y. Photocatalysis on Supported Gold and Silver Nanoparticles Under Ultraviolet and Visible Light Irradiation. *Green Chem.* **2013**, *15*, 1814−1833.

(29) Xiao, Q.; Jaatinen, E.; Zhu, H. Y. Direct Photocatalysis for Organic Synthesis Using Plasmonic Metal Nanoparticles Irradiated with Visible Light. *Chem.—Asian J.* **2014**, DOI: 10.1002/asia.201402310.

(30) Balamurugana, B.; Maruyama, T. Evidence of an Enhanced Interband Absorption in Au Nanoparticles: Size-Dependent Electronic Structure and Optical Properties. *Appl. Phys. Lett.* **2005**, *87*, 143105.

(31) Chen, Y.; Somsen, C.; Milenkovic, S.; Hassel, A. W. Fabrication of Single Crystalline Gold Nanobelts. *J. Mater. Chem.* **2009**, *19*, 924–927.

(32) Wu, X. F.; Darcel, C. Iron-Catalyzed One-Pot Oxidative Esterification of Aldehydes. *Eur. J. Org. Chem.* **2009**, 1144–1147.

(33) Suzuki, K.; Yamaguchi, T.; Matsushita, K.; Iitsuka, C.; Miura, J.; Akaogi, T.; Ishida, H. Aerobic Oxidative Esterification of Aldehydes with Alcohols by Gold–Nickel Oxide Nanoparticle Catalysts with a Core–Shell Structure. *ACS Catal.* **2013**, *3*, 1845–1849.

(34) Owston, N. A.; Nixon, T. D.; Parker, A. J.; Whittlesey, M. K.; Williams, J. M. J. Conversion of Primary Alcohols and Aldehydes Into Methyl Esters by Ruthenium-Catalysed Hydrogen Transfer Reactions. *Synthesis* **2009**, *9*, 1578–1581.

(35) Cano, I.; Chapman, A. M.; Urakawa, A.; van Leeuwen, P. W. N. M. Air-Stable Gold Nanoparticles Ligated by Secondary Phosphine Oxides for the Chemoselective Hydrogenation of Aldehydes: Crucial Role of the Ligand. *J. Am. Chem. Soc.* **2014**, *136*, 2520–2528.